sciendo

POLISH MARITIME RESEARCH 3 (115) 2022 Vol. 29; pp. 119-127
10.2478/pomr-2022-0032

NUMERICAL STUDY OF THE EJECTION COOLING MECHANISM OF VENTILATION FOR A MARINE GAS TURBINE ENCLOSURE

Hong Shi[1]*
Qianwei Zhang[1]
Meinan Liu[1]
Kaijie Yang[2]
Jie Yuan[2]
[1] Jiangsu University of Science and Technology; China
[2] Nanjing University of Aeronautics & Astronautics; China

* Corresponding author: *shihong@nuaa.edu.cn* (Hong Shi)

ABSTRACT

A marine gas turbine enclosure must be designed to prevent overheating of the electrical and engine control components as well as diluting potential fuel leaks. In order to achieve an optimal enclosure design, a numerical study of the ventilation-ejection cooling mechanism of a gas turbine enclosure is carried out in this paper. The evaluation index of the ejection cooling performance is first proposed and the algorithm of numerical simulation is verified. On this basis, orthogonal combinations of structural parameters are carried out for the expansion angle α of the lobed nozzle and the spacing S between the outlet plane of the lobed nozzle and the inlet plane of the mixing tube. The flow and the temperature distribution inside the enclosure are analysed under different operating conditions. The results show that the influence of the lobed nozzle expansion angle α and the spacing S on the performance is not a single-valued function but the two influencing factors are mutually constrained and influenced by each other. For any spacing, the combined coefficient is optimal for the expansion angle α = 30°. When the expansion angle α = 45° and the spacing S = 100 mm, the combined coefficient and the temperature distribution inside the enclosure are optimal at the same time.

Keywords: Gas Turbine Enclosure, Ejecting Cooling, Ventilation, CFD

INTRODUCTION

A large marine gas turbine is one of the important energy conversion and transfer devices for ships. Gas turbines can use different types of fuel and emit fewer pollutants [1]. In addition, the heat from gas turbine exhaust gas can be further utilised in the thermochemical reactor and steam generator, and the water extracted from the exhaust gas can be reused for steam injection in the gas turbine cycle [2-4]. All of this makes gas turbines for marine use more competitive. Presently, the most common large marine gas turbine is the General Electric LM2500, with subsequent modifications, such as the LM2500+ and LM2500+G4. The marine gas turbines have an enclosure design with mechanical drives and other auxiliary components inside the enclosure. The enclosure not only isolates and protects the gas turbine from the external environment, but also reduces the impact of gas turbine operating noise and allows for easy maintenance and storage [5-7]. However, the closed working environment also makes it necessary to design a ventilation and cooling system for the gas turbine enclosure, to boost the power and efficiency of the gas turbine [8].

The ventilation and cooling system of a marine gas turbine enclosure prevents overheating of electrical and engine control components, as well as diluting potential fuel leaks, to eliminate stagnant areas that could lead to ignition in the cowling [9,10]. Conversely, excessive ventilation airflow may not only lead to unnecessary engine heat loss and excessive auxiliary power

requirements [11], but it may also result in excessive mixing tube outlet flow rates and, thus, additional installation costs. Therefore, optimum design of the enclosure ventilation and cooling must be based on an appropriate ventilation flow rate and temperature distribution. Traditionally, forced cooling ventilation is mostly used for cooling the enclosure, with fans providing the appropriate ventilation flow at the air inlet, which has more energy consumption in marine use. In contrast to forced cooling ventilation, ejection cooling does not require the installation of special cooling equipment and can save space in the ship design. In addition, exhaust noise can be suppressed and the intensity of infrared radiation reduced when using ejector airflow to cool the enclosure. Therefore, ejection cooling will be more widely used in marine gas turbine enclosure ventilation systems in the future [12]. However, current scholarly research is focused on forced cooling ventilation. CFD (Computational Fluid Dynamics) numerical simulations and experiments are used to obtain the distribution of airflow velocity and temperature inside the enclosure, as well as airflow organisation in the event of a gas leak [13-15]. Although there are relatively few references on the use of ejection cooling to reduce the internal temperature of gas turbine enclosures, ejecting systems have been studied relatively extensively for other applications.

Numerous studies have focused on the design of the lobed nozzle ejector and its matching with the mixing tube. Maqsood and Birk [16,17] investigated the ejecting performance of a bent ejector with a long elliptical cross-sectional area, a subsonic air-air bending ejector and an annular induced diffuser. Hu et al. [18] used PIV experiments to investigate the vortex structure and degree of turbulence in the near field of an ejector caused by a lobed nozzle. The results showed that the laminar area of the lobed nozzle is shorter and the smaller scale turbulent structures appear earlier, and are more extensive, than in the circular nozzle. Nastase and Meslem [19] found that a lobed nozzle without an expansion angle allows the improvement of mixing in the generated stream compared to a circular ejector. A lobed nozzle with an expansion angle reaches four times the entrainment of a circular ejector. Sheng [20] investigated the effect of different lobed peak spoilers on ejector performance (such as the entrainment coefficient, mixing efficiency and total pressure recovery coefficient). Varga et al. [21] found that the nozzle outlet plane influences both the critical back pressure and the entrainment coefficient. An optimum distance exists between the nozzle outlet plane and the mixing tube inlet, to allow for maximum entrainment of the secondary stream.

In summary, the lobed nozzle ejector itself and the matching of the ejector with other devices has been relatively well studied by relevant scholars. Most of the research focuses on the optimisation of the entrainment coefficient, with the objective of reducing the mainstream temperature and weakening the infrared radiation intensity, and less on the temperature distribution and pressure loss within the enclosure assembly. Although the ejection cooling is mainly based on the ejecting principle, the design objective is not only to improve the air entrainment coefficient and reduce the total pressure loss of the ejection cooling system, but also to avoid localised high temperatures in the enclosure. Therefore, the results of the above-mentioned research on ejectors cannot be simply extended to the ventilation and cooling system of the gas turbine enclosure.

Accordingly, this paper takes a marine gas turbine enclosure as the research object and proposes evaluation indexes for the cooling performance of the enclosure. The orthogonal combination method is used to obtain the ejection cooling effect under different structure parameters. Furthermore, the mechanism analysis of the flow field and temperature distribution is carried out. Finally, the optimal ventilation and cooling solution is obtained, based on the multi-objective evaluation.

GEOMETRICAL AND METHODOLOGY

GEOMETRICAL MODEL AND BOUNDARY CONDITION

In this paper, the ejection cooling system of a marine gas turbine was studied and a geometrical model established. Due to the complexity of the actual model and the limitations of computing resources, the influence of the auxiliary equipment and the piping arrangement in the enclosure were not considered when building the geometrical model. Fig.1 shows a geometrical model reflecting the main features of the gas turbine casing.

The *Realizable k-ε* turbulence model was used in the CFD numerical simulation. Meanwhile, the equations of mass, momentum, turbulence kinetic energy and dissipation rate were solved using the SIMPLE (Semi-Implicit Method for Pressure Linked Equation) algorithm. The airflow properties were taken to be those for an ideal gas and the temperature was defined in sections, according to the state of the gas turbine operation. The surface of the high-temperature components of the gas turbine was coated with thermal protection material and the gas turbine casing set up as a slip-free wall, with an emissivity of 0.9 [22].

Furthermore, the exhaust plenum outlet was set up as a mass flow inlet with a mass flow rate of 27.8 kg/s and temperature of 782 K. The cooling inlet was set up as a pressure inlet with a temperature of 300 K and a pressure of 0 Pa. The mixing tube outlet was set up as a pressure outlet with a temperature of 300 K and a pressure of 1000 Pa.

Fig.2 shows the structure of the lobed nozzle ejector and the ejection cooling system.

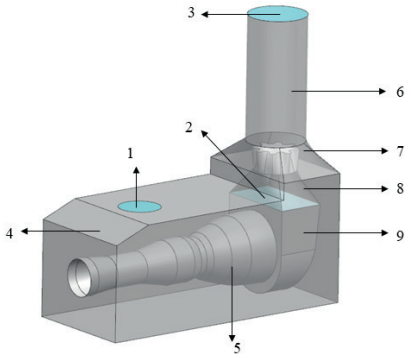

(a) Enclosure geometrical model:
1 - Cooling inlet (Secondary stream inlet);
2 - Exhaust plenum outlet (Mainstream inlet);
3 - Mixing tube outlet (Mixed streams outlet);
4 - Gas turbine enclosure;
5 - Gas turbine casing;
6 - Mixing tube;
7 - Transition section (Between the mixing tube and the enclosure);
8 - Lobed nozzle ejector;
9 - Exhaust plenum.

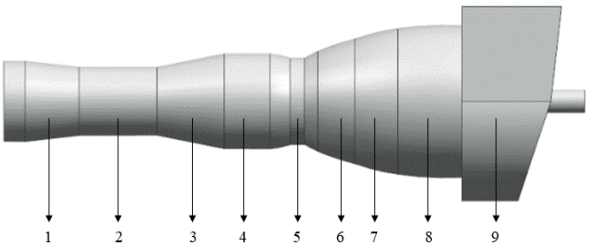

(b) Gas turbine casing geometrical model:
1 - Inlet section 350 K;
2 - Low pressure air compressor 400 K;
3 - High pressure air compressor 550 K;
4 - Combustion 600 K;
5 - Aft combustion chamber 500 K;
6 - Transition section700 K;
7 - Power turbine 400 K;
8 - Aft power turbine 400 K;
9 - Exhaust plenum 390 K.

Fig. 1. Geometrical model

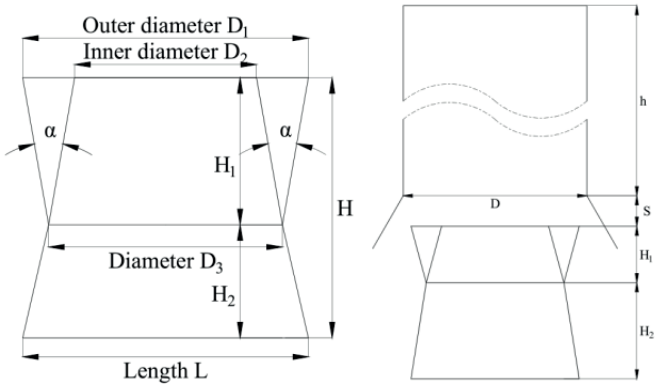

(a) Lobed nozzle ejector *(b) Ejection cooling system*

Fig. 2. Schematic of the structure

The lobed nozzle expansion angle α and the spacing S between the outlet of the lobed nozzle and the inlet of the mixing tube were set up as an orthogonal combination of structural parameters. Unlike traditional lobed nozzle ejectors, the lobed nozzle ejector studied in this paper consisted of a lobed nozzle section (H_1) and a square-to-circle section (H_2), as shown in Fig.2(a). As the exhaust plenum outlet plane is square, the lobed nozzle needed to be designed with a square-to-circle section, to connect the square plane of the exhaust plenum outlet to the circle plane at the bottom of the lobed nozzle.

It should be noted that, because the lobed nozzle ejector and the gas turbine enclosure were matched to each other, the total height (H) of the lobed nozzle ejector remained constant during the structural analysis of the lobed nozzle ejector. Therefore, when designing different expansion angles α by varying the lobed nozzle height (H_1), the change in lobed nozzle height (H_1) caused a change in the height of the square-to-circle height (H_2). There is a matching relationship between the two sections.

As shown in Fig.2(b), the spacing between the outlet of the lobed nozzle ejector and the inlet of the mixing tube is S. Specifically, S < 0 mm means that the ejector outlet is inside the mixing tube. S = 0 mm means that the ejector outlet is in the same plane as the mixing tube inlet. S > 0 mm means that there is a distance between the ejector outlet and the mixing tube inlet.

The fixed parameters of the ejector and mixing tube structure were designed as shown in Table.1.

Tab. 1. Fixed parameters

Design content			Parameter settings
Ejector	Ejector	Total height	1000 mm
	Lobed nozzle section (H_1)	Outlet area	591323 mm^2
		Width of the lobe	100 mm
		Outer diameter (D_1)/ Inner diameter (D_2)	D_1 = 1100 mm, D_2 = 700 mm
		Diameter of the bottom circular surface (D_3)	900 mm
		Number of the lobe	10 (Evenly distributed by circumference)
	Square-to-circle section (H_2)	Exhaust plenum outlet plane	1100 mm × 2000 mm
Mixing tube	Diameter (D)		1200 mm

Based on the fixed parameters in Table 1, orthogonal combinations were performed for four different lobed nozzle expansion angles α and six different spacings S, for a total of 24 combinations. Specifically, the expansion angle α of Case 1 - Case 6 was 20° and the spacings were: -100 mm, 0 mm, 100 mm, 200 mm, 400 mm, 500 mm, respectively. The expansion angle α for Case 7 - Case 12 was 30° and

the spacings were as above. The expansion angle α for Case 13 - Case 18 was 45° and the spacings were as before. The expansion angle α for Case 19 - Case 24 was 60° and the spacings were as above.

EVALUATION INDICATORS

System Performance Indicators

Due to space limitations in the ship, it is difficult to achieve the optimum mixing tube lengths for the ejector design. At the same time, considering the mixing loss between the mainstream and secondary streams, the maximum entrainment coefficient should not be pursued while meeting the cooling requirements of the gas turbine enclosure [23]. The entrainment coefficient and pressure are closely related to the temperature field. Therefore, in the actual program selection process, the flow field calculation can be performed first, to obtain a series of cases that meet the requirements, and then temperature field checks can be carried out. This method makes the calculation relatively efficient.

In this paper, the entrainment coefficient was combined with the pressure loss coefficient in the flow field calculation, to obtain the combined coefficient, and it was used as an evaluation indicator for the flow characteristics of the ejection cooling system. The implication of the combined coefficient is that a better system performance should provide a higher entrainment coefficient at a lower pressure loss. The equation is as follows:

$$Combined\ coefficient = \frac{Entrainment\ coefficient}{Pressure\ loss\ coefficient} \quad (1)$$

– Entrainment coefficient

The entrainment coefficient is a dimensionless coefficient that indicates the entrainment capacity of the ejection cooling system, and is defined as follows:

$$n = \frac{G_2}{G_1} \quad (2)$$

where G_1 is the mass flow rate of the mainstream, and G_2 is the mass flow rate of the secondary stream.

– Pressure loss coefficient

The pressure loss coefficient is a dimensionless coefficient which indicates the flow loss in the ejection cooling system and is expressed as follows:

$$\prod = \frac{P_1 - P_2}{q} \quad (3)$$

where P_1 is the total pressure at the outlet of the exhaust plenum, P_2 is the total pressure at the outlet of the mixing tube, and q is the dynamic pressure at the outlet of the exhaust plenum.

Temperature Indicators

The air temperature in a typical plane within the enclosure needs to be less than 82°C (355 K) during operations [24]. It should be noted that, due to the high temperature of the gas turbine casing, it is difficult to significantly reduce the temperature in the section near the gas turbine casing by ejection cooling alone. Therefore, the temperature in the section near the gas turbine casing does not have to be considered within the required temperature indicators.

ALGORITHM VALIDATION

In order to ensure the reliability of the numerical simulations in this paper, a geometric model was built based on the parameters in the literature [25]. For the numerical simulation, the experimental system was simplified and only the lobed nozzle section was retained, as shown in Fig.3. Specifically, the outer diameter of the outlet plane of the lobed nozzle is 108.0 mm, the inner diameter is 54.0 mm, and the diameter of the inlet plane is 70 mm. The height of the lobed nozzle is 73 mm, the width of each lobe is 7.2 mm, and the number of lobes is 12. The boundary conditions of the numerical simulation were based on the experiments in the literature. Specifically, the mainstream inlet was set as the velocity inlet with a velocity of 21 m/s and a temperature of 620 K. The secondary stream inlet and the mixing outlet were simultaneously set as pressure boundaries, with an ambient pressure and a temperature of 300 K. The results of the experiments and simulations are shown in Fig.4.

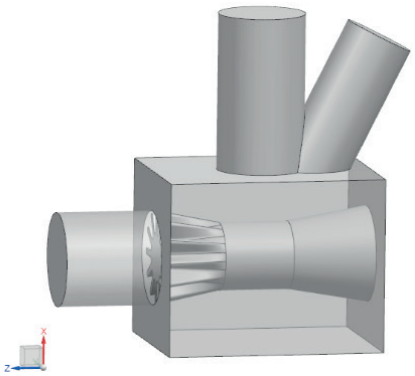

Fig. 3. Geometric model

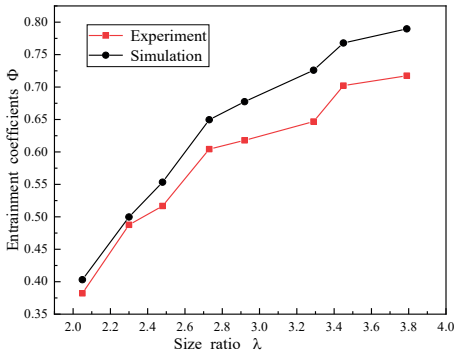

Fig. 4. Experiments and simulations

As shown in Fig.4, the simulation results are slightly higher than the experimental results. The main reason for this is that, in the experiments, the mainstream inlet of the lobed nozzle ejector is equipped with piping in front of it, which may lead to a non-uniform distribution of the mainstream velocity. In the simulations, however, the mainstream velocity is designed to be uniformly distributed. Therefore, there is a difference between the simulated and experimental mainstream inlets. Because the difference in the results of the entrainment coefficient in the experiments and simulations is less than 10%, for different size ratios, and the variation trend is relatively consistent, the numerical simulation of the ejector (in this paper) has some reliability and can be used for subsequent studies.

MESH INDEPENDENCE

An unstructured polyhedral mesh was created for the geometric model, with mesh refinement in more complex areas, such as the inlet and outlet of the model and the lobed nozzle ejector. At the same time, a boundary layer was created on the mixing tube and the gas turbine casing. In order to ensure that the results were independent of the number of meshes, when analysing the performance of the system, the geometric model of Case 3 (α = 20°, S = 100 mm) was chosen to create meshes of five different diameters. The effect of different diameters of meshes on the performance of the system was analysed using the total pressure of the mainstream inlet and the average temperature of the central plane as indicators. The results are shown in Table 2.

Tab. 2. Mesh independence validation

Number of meshes	2.05 million	3.37 million	4.70 million	5.88 million	6.75 million
Total pressure of the mainstream inlet (Pa)	3549.7	3684.4	3744.3	3748.4	3746.9
Average temperature of the central plane (K)	313.4	315.1	315.6	315.7	315.6

As shown in Table 2, when the number of meshes reaches 4.70 million, the total pressure at the mainstream inlet and the average temperature at the central plane hardly change as the mesh number increases. Considering the speed of the simulation and the accuracy of the results, a mesh with the number of 4.70 million was chosen for the subsequent simulations in this paper.

SIMULATION AND RESULTS

COMBINED COEFFICIENT

Fig.5 shows the variation pattern of the combined coefficient with the lobed nozzle expansion angle α and spacing S.

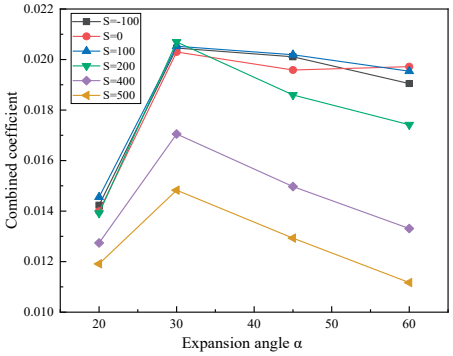

Fig. 5. Combined coefficient variation pattern

As shown in Fig.5, with the increase of the expansion angle α, the combined coefficient first increases and then decreases. When the expansion angle α = 20°, the ejector structure results in a high total pressure loss and, therefore, the combined coefficient remains low. For any spacing, the combined coefficient is optimal for the expansion angle α = 30°. Of the 24 cases, the four cases with the best combined coefficients are Case 7 (α = 30°, S = -100 mm), Case 9 (α = 30°, S = 100 mm), Case 10 (α = 30°, S = 200 mm), and Case 15 (α = 45°, S = 100 mm), with Case 10 having the best combined coefficient of them all. The following is a specific analysis, in terms of both the entrainment coefficient and the pressure loss coefficient.

Entrainment Coefficient

Fig.6 shows the variation pattern of the entrainment coefficient with the expansion angle α and spacing S.

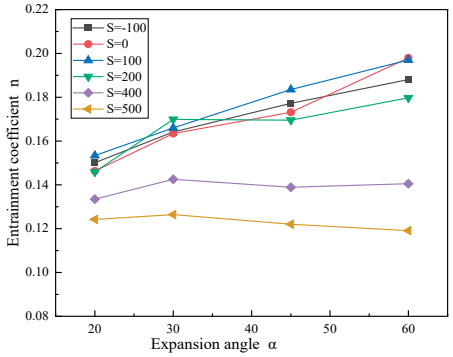

Fig. 6. Entrainment coefficient variation pattern

From Fig.6, it can be seen that there are two trends in the entrainment coefficient, with different expansion angles α and spacing S.

(1) When the spacing S ≤ 100 mm, the entrainment coefficient increases with increasing expansion angle α.

In order to further study the mechanism of the effect of the expansion angle α on the entrainment coefficient, the velocity distribution and stream-wise vortices are specifically analysed for a spacing S = 0 mm. Fig.7 shows the velocity distribution of the ejector.

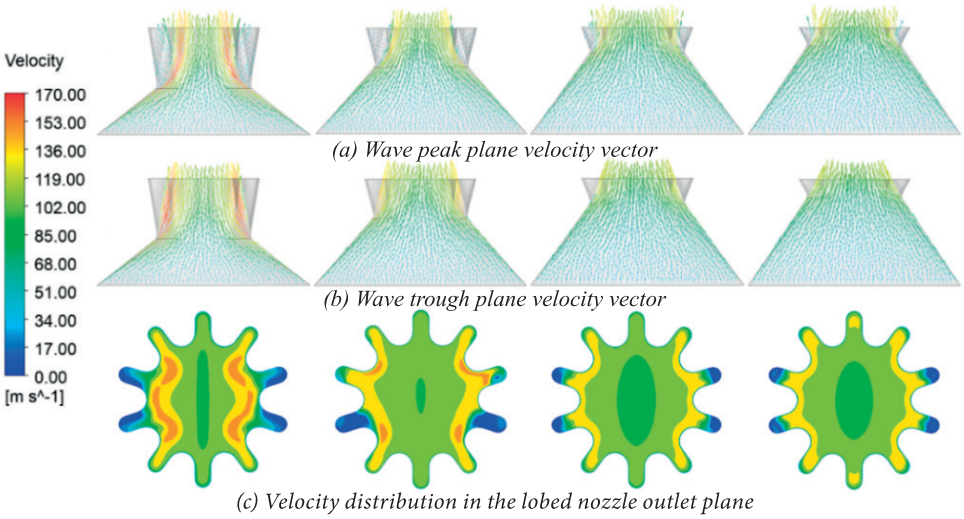

(a) Wave peak plane velocity vector

(b) Wave trough plane velocity vector

(c) Velocity distribution in the lobed nozzle outlet plane

Fig. 7. Velocity of the lobed nozzle ejector plane (From left to right : 20°, 30°, 45°, 60°)

As shown in Fig.7, due to the influence of the square-to-circle section (H_2) of the ejector, the mainstream velocity distribution within the ejector is not uniform and localised high velocity areas can exist near the walls. When the expansion angle α = 20°, the height of the square-to-circle section (H_2) is the smallest, the deformation in the length direction is the most intense, and the backflow area at the lobe boundary is larger. As the expansion angle α increases, the height of the square-to-circle section (H_2) gradually increases, and the deformation between the length direction of the exhaust plenum outlet and the circle plane at the bottom of the lobed nozzle is gradually eased. Meanwhile, the velocity of the mainstream gradually decreases along the walls and the velocity distribution inside the ejector tends to be uniform. In addition, as the height of the lobed nozzle section (H_1) gradually decreases, the backflow area within the lobed nozzle also gradually decreases and the utilisation of the mainstream gradually increases. Thus, as the expansion angle α increases, the entrainment coefficient gradually rises.

(2) When the spacing S ≥ 200 mm, the entrainment coefficient fluctuates with increasing expansion angle α.

Taking the expansion angle α = 45° as an example, Fig.8 shows the velocity vector in the inlet area of the mixing tube for spacings of 200 mm, 400 mm, and 500 mm.

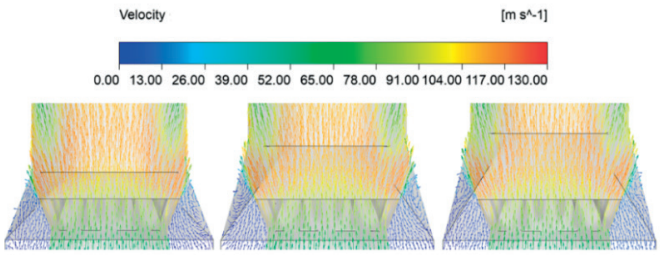

Fig. 8. Velocity vector in the mixing tube inlet area (From left to right : 200 mm, 400 mm, 500 mm)

As shown in Fig.8, when the spacing S = 200 mm, the mainstream begins to diffuse fully as it reaches the mixing tube inlet, with a small proportion of the mainstream impacting the wall of the transition section in front of the mixing tube inlet. These block the passage of the secondary stream into the mixing tube and the wall of the transition section has an inclined angle, which causes the secondary stream to randomly return to the interior of the enclosure, thus reducing the entrainment coefficient. When the expansion angle α changes, the impact point of the mainstream and transition section changes, resulting in fluctuations in the entrainment coefficient. However, when the spacing S = 200 mm, there is relatively little backflow and so the entrainment coefficient remains at a high level.

As the spacing S increases further, the passage from the ejector outlet plane to the inlet plane of the mixing tube gradually widens and the mainstream is fully diffused before it reaches the inlet of the mixing tube. The impact of the mainstream on the transition section wall reduces the utilisation of the mainstream and blocks the passage of the secondary stream, making the backflow of the secondary stream more serious. Therefore, the entrainment coefficient is generally low when the spacing S is large. The degree of backflow and passage blockage of the secondary stream depends on the matching relationship between the expansion angle α and the mixing tube. As the structure of the ejector and the transition section in front of the mixing tube do not vary in a univariate manner, the entrainment coefficient fluctuates with the expansion angle α, but does not vary significantly.

Pressure Loss Coefficient

Fig.9 shows the variation pattern of the pressure loss coefficient with the lobed nozzle expansion angle α and the spacing S.

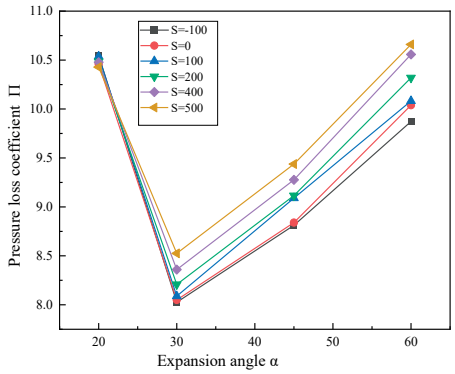

Fig. 9. Pressure loss coefficient variation pattern

As can be seen from Fig. 9, the pressure loss coefficient follows the same trend at different spacings. This means that, as the expansion angle α increases, the pressure loss coefficient at any spacing S shows a tendency to decrease and then increase. Specifically, the pressure loss coefficient decreases rapidly as the expansion angle α increases from 20° to 30°. As the expansion angle α increases further, the pressure loss coefficient gradually increases.

In order to further study the mechanism of the effect of the expansion angle α on the pressure loss coefficient, a pressure loss table is presented, for specific analysis. Using the spacing S = 0 mm as an example, Table 3 shows the total pressure loss of the ejection cooling system.

Tab. 3. Total pressure loss in the ejection cooling system

Spacing (S) / mm	Expansion angle (α)	Total pressure loss inside the ejector / Pa			Total pressure loss in the ejection cooling system / Pa		
		Lobed nozzle section (H_1)	Square-to-circle section (H_2)	Total pressure loss	Exhaust plenum outlet plane	Mixing tube outlet plane	Total pressure loss
0	20°	553.49	400.08	953.57	3719.74	1910.49	1809.25
	30°	303.87	164.73	468.60	3418.68	1923.11	1495.57
	45°	295.37	124.29	419.66	3454.36	1932.77	1521.59
	60°	327.39	100.80	428.19	3693.55	1971.37	1722.18

As can be seen from Table 3, two important mechanisms contribute to the total pressure loss in the ejector. These are: non-uniformity of the mainstream velocity, due to the sharp geometrical deformation of the square-to-circle part (H_2) of the ejector, and intense mixing, due to the enhanced entrainment capacity. Specifically, as the expansion angle α increases, the total pressure loss in the square-to-circle section (H_2) gradually decreases. At an expansion angle α = 20°, the total pressure loss in the square-to-circle section (H_2) is the highest, at approximately 400.08 Pa. The main reason for this is that the square-to-circle section (H_2) achieves a sharp square to circle transition at a relatively short height. The large change in geometry leads to a non-uniform mainstream velocity which, in turn, leads to large pressure loss. As the square-to-circle section (H_2) gradually increases, the deformation is gradually eased and the local pressure loss is reduced. However, when the expansion angle α = 60°, the entrainment capacity increases significantly and the energy consumed by the entrained secondary stream also increases significantly, resulting in a higher total pressure loss in the lobed nozzle section (H_1).

TEMPERATURE DISTRIBUTION

For the study of the gas turbine ejection cooling system, in addition to obtaining a better combined coefficient, it is equally important to reduce the high temperature areas inside the enclosure. Therefore, this section provides a specific analysis of the temperature distribution in typical planes inside the enclosure for the four cases with the better combined coefficients. Fig.10 shows the temperature distribution in typical planes inside the enclosure for each of the four cases.

As shown in Fig.10, the airflow enters the enclosure from the cooling inlet and flows to the gas turbine casing surface and, subsequently, along the gas turbine surface below. Therefore, the temperature of the airflow directly below the cooling inlet is lower. As the space inside the enclosure increases, the airflow velocity gradually decreases and, combined with the radiation from the high temperature of the gas turbine casing surface, the airflow is further heated inside the enclosure.

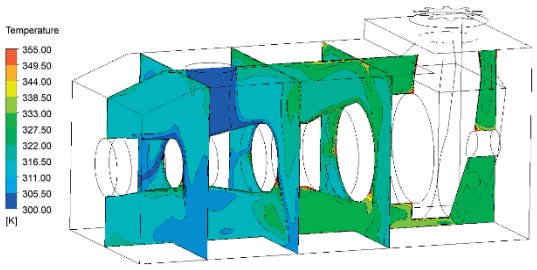

Case 7 (α = 30°, S = -100 mm)

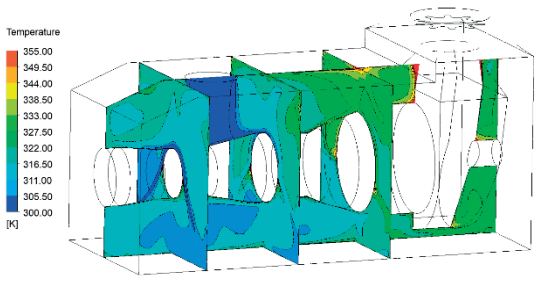

Case 9 (α = 30°, S = 100 mm)

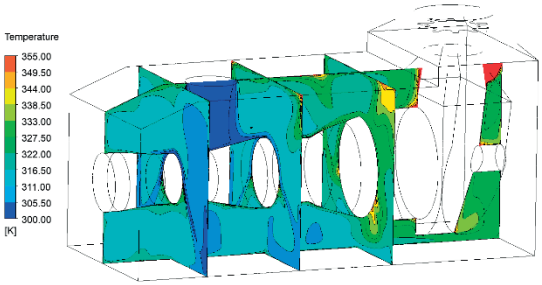

Case 10 (α = 30°, S = 200 mm)

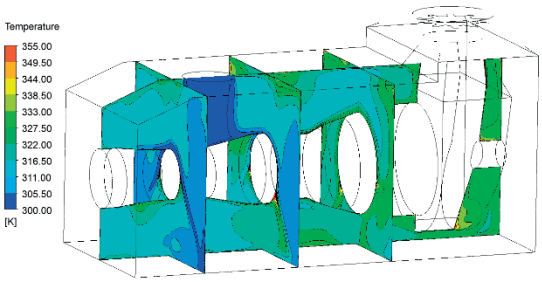

Case 15 (α = 45°, S = 100 mm)

Fig. 10. Temperature distribution in typical planes

However, in Case 7, Case 9 and Case 10, there are localised areas with high temperatures on the top wall of the enclosure. This is because, as the spacing S increases, the backflow near the ejector inside the enclosure gradually becomes more serious. At the same time, more high temperature areas are generated inside the enclosure. In Case 15, the relatively high entrainment coefficient results in relatively high airflow velocities inside the enclosure and a relatively low temperature in the enclosure, with no high temperature areas inside the enclosure. On balance, Case 15 is the preferred option.

CONCLUSION

In this paper, a numerical study was carried out on the ventilation and cooling system of a gas turbine enclosure. The analysis focused on the effects of different expansion angles α and the spacing S between the lobed nozzle outlet plane and the mixing tube inlet plane on the ventilation and cooling performance. The combined coefficients of the ejection cooling system and the temperature distribution inside the enclosure under different design parameters were obtained and analysed specifically. The specific findings of this paper are as follows.

(1) The influence of the expansion angle α and the spacing S on performance is not a single-valued function, but the two influencing factors are mutually constrained and influenced by each other. The main reason for this is that the mixing tube in the enclosure and the square-to-circle section (H_2) interfere with the performance of the ejector, which differs significantly from a conventional ejector.

(2) The sharp reduction in height of the square-to-circle section (H_2) leads to the existence of a low velocity backflow area in the lobed nozzle, causing a blocking effect on the mainstream. However, as the expansion angle α increases, the backflow area within the lobed nozzle gradually decreases, and the utilisation of the mainstream gradually increases, more secondary streams can be entrained.

(3) For any spacing, the optimal combined coefficient is obtained for an expansion angle α = 30°. However, in the case of the better solution, there may still be localised high temperature areas inside the enclosure. So, four cases with the best combined coefficients are selected before the local temperature distribution analysis, namely Case 7, Case 9, Case 10 and Case 15. Through comparison and analysis, Case 15 has a better combined coefficient and there are no high temperature areas inside the enclosure, therefore Case 15 is the preferred option.

REFERENCES

1. N.R. Ammar and A. Farag, "CFD Modeling of Syngas Combustion and Emissions for Marine Gas Turbine Applications" Polish Maritime Research, vol.23, no.3, pp.39-49, 2016. doi: 10.1515/pomr-2016-0030.
2. O. Cherednichenko, S. Serbin, and M. Dzida, "Application of Thermo-chemical Technologies for Conversion of Associated Gas in Diesel-Gas Turbine Installations for Oil and Gas Floating Units," Polish Maritime Research, vol. 26, no. 3, 2019. doi: 10.2478/pomr-2019-0059.
3. S. Serbin, K. Burunsuz, M. Dzida, J. Kowalski, and D. Chen, "Investigation of Ecological Parameters of a Gas Turbine Combustion Chamber with Steam Injection for the Floating Production, Storage, and Offloading Vessel," International Journal of Energy and Environmental Engineering, 2021. doi: 10.1007/s40095-021-00433-w.
4. S. Serbin, N. Washchilenko, M. Dzida, and J. Kowalski, "Parametric Analysis of the Efficiency of the Combined Gas-Steam Turbine Unit of a Hybrid Cycle for the FPSO Vessel," Polish Maritime Research, vol. 28, no. 4, 2022. doi: 10.2478/pomr-2021-0054.
5. O. Kyrylash, V. Kostiuk, A. Smirnov, D. Tkachenko, and I. Loboda, "Mathematical Simulation of the Gas Turbine Packages Thermal State." Proceedings of the ASME Turbo Expo 2018: Turbomachinery Technical Conference and Exposition. vol.5C, Oslo, Norway. June 11-15, 2018. doi: 10.1115/GT2018-77194.
6. J. Kowalski, F. Di Mare, S. Theis, A. Wiedermann, M. Lange, and R. Mailach, "Investigation of the Ventilation Flow in a Gas Turbine Package Enclosure." European Conference on Turbomachinery Fluid Dynamics and Thermodynamics, 2019. doi: 10.29008/ETC2019-438.
7. A. Corsini, G. Delibra, M. Giovannelli, G. Lucherini, S. Minotti, S. Rossin, and L. Tieghi, «Prediction of Ventilation Effectiveness for LM9000 Package with Machine Learning.» Proceedings of the ASME Turbo Expo 2020: Turbomachinery Technical Conference and Exposition. vol.9. Virtual, online. September 21-25, 2020. doi: 10.1115/GT2020-14916.
8. Z. Domachowski, and M. Dzida, "Applicability of Inlet Air Fogging to Marine Gas Turbine" Polish Maritime Research, vol.26, no.1, pp.15-19, 2019. doi: 10.2478/pomr-2019-0002.
9. International Standard ISO 21789:2009 Gas Turbine Applications – Safety, International Organisation for Standardization, 2009.
10. G. Lucherini, V. Michelassi, and S. Minotti, "The Impact of Model Assumptions on the CFD Assisted Design of Gas Turbine Packages." Proceedings of the ASME Turbo Expo 2019: Turbomachinery Technical Conference and Exposition. vol.9. USA. June 17-21, 2019. doi: 10.1115/GT2019-90871.
11. R. Yerram, R. Watkins, and B. Ponnuraj, "Aeroderivative Gas Turbine Enclosure Ventilation System." Proceedings of the ASME Turbo Expo 2021: Turbomachinery Technical Conference and Exposition. vol.2C. Virtual, online. June 7-11, 2021. doi: /10.1115/GT2021-59136.

12. D.M. Li, L. Wang, X.Y. Wen, and S.D. Cao, "Numerical Simulation and Experimental Study of Marine Combustion Engine Exhaust Ejector." Thermal Power Engineering, vol.17, no.3, pp.226-230, 2002. doi: 10.3969/j.issn.1001-2060.2002.03.002.

13. B. Ponnuraj, B. Sultanian, A. Novori, and P. Pecchi, "3D CFD Analysis of an Industrial Gas Turbine Compartment Ventilation System." Proceedings of the ASME 2003 International Mechanical Engineering Congress and Exposition. Heat Transfer, vol.2. Washington, DC, USA. November 15–21, 2003. pp. 67-76. ASME. doi: 10.1115/IMECE2003-41672.

14. E. Graf, T. Luce, and F. Willett, "Design Improvements Suggested by Computational Flow and Thermal Analyses for the Cooling of Marine Gas Turbine Enclosures." Proceedings of the ASME Turbo Expo 2005: Power for Land, Sea, and Air. vol.5. Reno, Nevada, USA. June 6-9, 2005. pp. 587-593. doi: 10.1115/GT2005-68574.

15. G. Lucherini, S. Minotti, G. Ragni, and F. Bologna, "Experimental and Numerical Investigation on Gas Turbine Package Scale Model." Proceedings of the ASME Turbo Expo 2018: Turbomachinery Technical Conference and Exposition. vol.9. Oslo, Norway. June 11-15, 2018. doi: 10.1115/GT2018-75694.

16. A. Maqsood, and A.M. Birk, "Effect of a Bend on the Performance of an Oblong Ejector." Proceedings of the ASME Turbo Expo 2007: Power for Land, Sea, and Air. vol.6. Montreal, Canada. May 14-17, 2007. pp.37-45. doi: 10.1115/GT2007-27851.

17. A. Maqsood, and A.M. Birk, "Effect of Entraining Diffuser on the Performance of Bent Exhaust Ejectors." Proceedings of the ASME Turbo Expo 2010: Power for Land, Sea, and Air. vol.7. Glasgow, UK. June 14-18, 2010. pp.2793-2802. doi: 10.1115/GT2010-23499.

18. H. Hu, T. Saga, T. Kobayashi, and N. Taniguchi, "Research on the Vortical and Turbulent Structures in the Lobed Jet Flow Using Laser Induced Fluorescence and Particle Image Velocimetry Techniques." Measurement Science & Technology, vol.11, no.6, p.698, 2000. doi: 10.1088/0957-0233/11/6/313.

19. I. Nastase and A. Meslem, "Passive Control of Jet Flows Using Lobed Nozzle Geometries." Mecanique Et Industries, vol.8, no.2, pp.101-109, 2007. doi: 10.1051/meca:2007027.

20. Z.Q. Sheng, "Jet Mixing of Lobed Nozzles with Spoilers Located at Lobe Peaks." Applied Thermal Engineering, vol.119, pp.165-175, 2017. doi: 10.1016/j.applthermaleng.2017.03.048.

21. S. Varga, A.C. Oliveira, and B. Diaconu, "Influence of Geometrical Factors on Steam Ejector Performance – A Numerical Assessment." International Journal of Refrigeration, vol.32, no.7, pp.1694-1701, 2009. doi: 10.1016/j.ijrefrig.2009.05.009.

22. Z.B. Zhang, X.Y. Zhang, B.B. Li, and P. Sun, "Optimal Design of Cooling Structure of an Industrial Type Gas Turbine Enclosure Mount." Thermal Science and Technology, vol.5, no.7, 2016. doi: 10.13738/j.issn.1671-8097.2016.05.013.

23. Y.L. Han, "Numerical Simulation and Experimental Study of Marine Gas Turbine Exhaust Ejector." Diss. Harbin Engineering University, 2005, doi: 10.7666/d.y780039.

24. H. Bagheri and D. Vahidi, "Ventilation of Gas Turbine Package Enclosures: Design Evaluation Procedure." 25th International Conference on Offshore Mechanics and Arctic Engineering, 2006.

25. Y.H. Liu, "Experimental Study and Numerical Simulation of Wave Flap Induced Mixer in Hot and Cold State." Diss. Nanjing University of Aeronautics and Astronautics, 2000. doi: 10.7666/d.y400568.

CONTACT WITH THE AUTHORS

Hong Shi

Jiangsu University of Science and Technology;
College of Energy & Power Engineering; Zhenjiang,
China

Qianwei Zhang

Jiangsu University of Science and Technology;
College of Energy & Power Engineering; Zhenjiang,
China

Meinan Liu

Jiangsu University of Science and Technology;
College of Energy & Power Engineering; Zhenjiang,
China

Kaijie Yang

Nanjing University of Aeronautics & Astronautics;
Key Laboratory of Aircraft environment control
and life support, MIIT; Nanjing,
China

Jie Yuan

Nanjing University of Aeronautics & Astronautics;
Key Laboratory of Aircraft environment control
and life support, MIIT; Nanjing,
China